Virtual Optimization of Nasal Insulin Therapy Predicts Immunization Frequency to Be Crucial for Diabetes Protection

Georgia Fousteri,[1] Jason R. Chan,[2] Yanan Zheng,[2] Chan Whiting,[2] Amy Dave,[1] Damien Bresson,[1] Michael Croft,[1] and Matthias von Herrath[1]

OBJECTIVE—Development of antigen-specific strategies to treat or prevent type 1 diabetes has been slow and difficult because of the lack of experimental tools and defined biomarkers that account for the underlying therapeutic mechanisms.

RESEARCH DESIGN AND METHODS—The type 1 diabetes PhysioLab platform, a large-scale mathematical model of disease pathogenesis in the nonobese diabetic (NOD) mouse, was used to investigate the possible mechanisms underlying the efficacy of nasal insulin B:9-23 peptide therapy. The experimental aim was to evaluate the impact of dose, frequency of administration, and age at treatment on Treg induction and optimal therapeutic outcome.

RESULTS—In virtual NOD mice, treatment efficacy was predicted to depend primarily on the immunization frequency and stage of the disease and to a lesser extent on the dose. Whereas low-frequency immunization protected from diabetes atrributed to Treg and interleukin (IL)-10 induction in the pancreas 1–2 weeks after treatment, high-frequency immunization failed. These predictions were confirmed with wet-lab approaches, where only low-frequency immunization started at an early disease stage in the NOD mouse resulted in significant protection from diabetes by inducing IL-10 and Treg.

CONCLUSIONS—Here, the advantage of applying computer modeling in optimizing the therapeutic efficacy of nasal insulin immunotherapy was confirmed. In silico modeling was able to streamline the experimental design and to identify the particular time frame at which biomarkers associated with protection in live NODs were induced. These results support the development and application of humanized platforms for the design of clinical trials (i.e., for the ongoing nasal insulin prevention studies).
***Diabetes* 59:3148–3158, 2010**

Type 1 diabetes is a complex and multifactorial autoimmune disease, in which, (pro-) insulin-specific T-cell responses have been described in lymphocytes obtained from nonobese diabetic (NOD) mice and (pre-)diabetic patients (1–4). In NOD mice, the insulin B:9-23 peptide sequence is a dominant epitope, and a single amino acid substitution in position 16 (B16:A) confers protection from the disease (5–7). Antigen-specific immunotherapies with whole insulin and B:9-23 peptide have been successful in preventing diabetes in NOD mice when administered via the subcutaneous, oral, or nasal route or via intramuscular DNA vaccination (8–18). The success in halting disease progression in prediabetic mice prompted physicians to establish similar protocols to test safety and efficacy in human prediabetic or diabetic subjects. To this end, clinical trials with nasal or oral whole insulin were conducted, which proved to be safe. However, diabetes progression was only slightly affected in a subset of insulin antibody–positive patients treated with oral insulin in the Diabetes Prevention Trial–Type 1 (19–24). In contrast, nasal insulin phase I–II trials in Finland (21,24) and in Australia (20), during which insulin was administered daily, failed to provide therapeutic efficacy. Highlighting the difficulties we are facing to rationally translate antigen-specific therapies to humans, there are conflicting reports on the efficacy of nasal B:9-23 peptide immunization in the NOD mouse. Taken together, these studies suggest that the manner by which insulin therapy is administered is important (25,26). Many variables may influence efficacy, including dose, frequency of administration, and the stage of the disease. Systematic investigation of each of these variables and combinations thereof is experimentally impractical because of the time constraints of in vivo studies, therefore necessitating biosimulation approaches.

The type 1 diabetes PhysioLab platform is a top-down, outcome-focused, large-scale mathematical model composed of ordinary differential and algebraic equations (27,28). This model reproduces type 1 diabetes pathogenesis in female NOD mice from birth until disease onset, with extensive representation of critical biological processes that were described in the literature and take place in the pancreas, the pancreatic-draining lymph nodes (PDLN), the gut, the nasal-associated lymphoid tissue (NALT), and the peripheral blood.

In the present study, we used a cohort of virtual NOD mice (VM) with diversity in underlying pathophysiology to investigate how variations in dose, frequency, and age at treatment initiation may impact the efficacy of nasal B:9-23 peptide therapy. The VM program was designed based on the following assumptions: *1*) induction of Treg is beneficial for disease prevention, *2*) induction of Th1 responses (interferon [IFN] γ) is detrimental for diabetes progression, whereas *3*) induction of Th2 responses (interleukin [IL]-10 and IL-4) favor disease protection. In silico investigation of the underlying mechanisms predicted that too frequent nasal B:9-23 immunization would inhibit IL-10 induction and the generation of adaptive Treg (aTreg),

From the [1]Diabetes Center, La Jolla Institute for Allergy and Immunology, La Jolla, California; and [2]Entelos, Foster City, California.
Corresponding authors: Jason R. Chan, chan@entelos.com, and Matthias von Herrath, matthias@liai.org.
Received 21 May 2010 and accepted 13 September 2010. Published ahead of print at http://diabetes.diabetesjournals.org on 23 September 2010. DOI: 10.2337/db10-0561.
G.F. and J.R.C. contributed equally to this work.

which should be critical in mediating protection. The model also aided in defining the optimal time frame in which Treg and IL-10 would be induced after immunization, thereby mapping the timing for both as crucial biomarkers.

Laboratory experiments confirmed many of these predictions, establishing immunization frequency and induction of IL-10$^+$ Treg as important considerations for the design of future clinical trials. Interestingly, in the initial and follow-up Peakman studies (2,29), it became evident that naturally occurring circulating islet-specific IL-10–producing cells regulate proinflammatory Th1 responses in healthy individuals by linked suppression. This suggests than in certain circumstances, given the heterogeneity of human type 1 diabetes, IL-10 production could be sufficient in sustaining prolonged antigen-specific tolerance. Future and ongoing trials might benefit from less frequent immunization, for example the ongoing nasal insulin studies in Australia (20). Moving forward, better defining the immunological parameters that could serve as biomarkers is of particular importance for improving the previously failed clinical trials (19–23,30) and for increasing the chance of success (31,32).

RESEARCH DESIGN AND METHODS

Pharmacokinetic modeling of B:9-23 therapy. The pharmacokinetic (PK) profile for nasal B:9-23 in the blood and NALT was approximated using published data for nasal delivery of the Ac1-9 peptide, used to induce tolerance in murine experimental autoimmune encephalomyelitis (33).

VM. VM were generated and validated as previously described (28). Briefly, individual VM were generated to represent variations in underlying physiology (supplementary Table 1, available at http://diabetes.diabetesjournals.org/cgi/content/full/db10-0561/DC1) by adjusting parameters representing various physiological processes. VM were then tested against a panel of internal validation protocols. Where necessary, parameter values were adjusted so appropriate behaviors to internal validation protocols were achieved. VM were considered valid if no further adjustments were necessary to pass a series of external validation protocols.

Experimental wet-lab NOD mice. NOD/LtJ female mice were purchased from The Jackson Laboratories (Bar Harbor, ME) and maintained in the La Jolla Institute for Allergy and Immunology under pathogen-free conditions and handled in accordance with protocols approved by the organization's animal care and use committee.

Glucose monitoring. Blood glucose was monitored weekly with the One-Touch Ultra (LifeScan, Milpitas, CA) monitoring system. Diabetes was defined as two consecutive blood glucose values >16.67 mmol/l.

B:9-23 peptide treatments. Amino acid sequence: SHLVEALYLVCGERG was purchased from Abgent (San Diego, CA) with >95% purity. Nasal administration: B:9-23 was diluted in sterile 1× PBS before given in the mouse nostril. Nasal immunization started either at 4 or 9 weeks of age, and two protocols were followed (high-frequency: 4, 9, 10, 11, 12, and 13 weeks of age and low-frequency: 4, 9, and 13 weeks of age). In some cases, the peptide was repeatedly given after 13 weeks of age every 4 weeks. The peptides were administered at each indicated time point for 3 consecutive days.

Intra-islet T-cell purification. Pancreata were digested with collagenase P (Roche Molecular Diagnostics, Pleasanton, CA), and islets were separated on a ficoll gradient (Histopaque 1077; Sigma-Aldrich, St. Louis, MO). Next, islets were dissociated into single cells. A mixture of islet cells and lymphocytes was used for further analysis.

Flow cytometry. Single-cell suspensions, after a 2.4G2 blocking step, were stained with the directly conjugated antibodies: CD4-Pacific blue, CTLA-4-PE, CD25-FITC, and CD127-PeCy7 (BD Pharmingen, Biolegend, or eBioscience, San Diego, CA) (isotype controls for all antibodies were included). For intracellular Foxp3 detection, cells were fixed with Fix/Perm buffer and stained with anti–Foxp3-APC (eBioscience). Cells were acquired on a LSRII flow cytometer (BD Biosciences) and analyzed using FlowJo software (Treestar, Ashland, OR).

Assessment of cytokine production by single lymphoid cells (ELIspot). IL-10, IL-4, and IFNγ (BD Pharmingen and Biolegend) produced by lymphocytes were detected by ELIspot as previously described (34).

Histology. Pancreata were immersed in Tissue-Tek OCT (Bayer, Torrance, CA) and quick frozen on dry ice, and 6-μm tissue sections were prepared. Sections were stained for insulin and CD4 or CD8 as previously described (34). To detect Foxp3 by immunofluorescence (IFS), primary antibody (anti–Foxp3-FITC, clone FJK-16s [4 mg/ml]) was used and amplified with Alexa 488 rabbit anti-fluorescein (12.5 mg/ml) and Alexa 488 goat anti-rabbit (7.5 mg/ml). To detect CD4, anti–CD4 biotin (3 mg/ml) followed by Alexa 647–conjugated streptavidin (1/1,000) was used. After fixation with 4% paraformaldehyde, insulin was detected with polyclonal guinea pig anti-swine insulin (1/140) followed by Alexa fluor 594–conjugated anti–guinea pig (1/1,000) (35). Slides were mounted with Slowfade Gold Antifade Reagent and visualized under a Nikkon Marianas microscope. Insulitis scoring was performed as previously described (34).

Antibody treatments. Anti–IL-10 (clone JES5-2A5) was purchased from BD Pharmingen. Antibody-treated or control (IgG isotype treated) mice received 125 μg of antibody intreperitoneally twice at 5, 6, 10, 11, 14, and 15 weeks of age. Mice received a total of 12 antibody injections.

Intracellular cytokine staining and adoptive transfer experiments. CD8-depleted lymphocytes from >30-week-old nasal B:9-23–treated normoglycemic mice were cultured with 10 μg/ml B:9-23 in the presence of 50 units/ml rhIL-2 for 3 days. Next, cells were either stimulated with 5 and 2.5 μg/ml plate bound anti-CD3 and soluble anti-CD28, respectively, or 10 μg/ml B:9-23 with or without 50 units/ml rhIL-2 before being assayed for intracellular cytokine staining with the BD cytofix/cytoperm kit. After B:9-23/IL-2 stimulation, cells were collected using the mouse IL-10 secretion assay (Miltenyi Biotech, Auburn, CA) according to the manufacturer's protocol. Approximately 1×10^6 IL-10$^+$ or IL-10$^-$ purified lymphocytes were adoptively transferred intravenously into 6- to 8-week-old not previously manipulated NOD mice.

Statistical analysis. Data are expressed as a means ± SD. The statistical significance of the difference between means was determined using the two-tailed Student t test or the log-rank test. *$P < 0.05$; **$P < 0.01$; ***$P < 0.005$.

RESULTS

Unexplained divergences in efficacy with various therapeutic nasal B:9-23 regimens. Nasal B:9-23 peptide therapy has been used with mixed efficacy to induce tolerance in prediabetic NOD mice. A comparison of all published protocols shows differences in dose and frequency of administration. Daniel et al. (9) showed that 40 μg of B:9-23 given over 3 consecutive days at 4 weeks of age and then again every 4 weeks beginning at 9 weeks of age induced tolerance. By contrast, Kobayashi et al. (12) did not observe efficacy when 20 μg of the peptide was given over 5 consecutive days at 4 weeks of age and then once a week for 5 weeks thereafter. Because the impact of age at treatment initiation had not been assessed in either of these studies, and to obtain further constraints for the modeling effort, we used one additional protocol. In these experiments, nasal B:9-23 therapy failed to confer protection at two different doses (40, 100 μg/mouse) when immunizations were started in 10-week-old mice (Fig. 1*A* and *B*). The complex differences between these immunization protocols provided the rationale for computer modeling to more precisely define our experimental options.

Impact of dose and age at treatment initiation on the efficacy of nasal B:9-23 peptide therapy. VM were calibrated to capture the above-described wet-lab experiments including the Daniel and Kobayashi protocols (supplementary Table 1). Subsequently, this VM cohort was used to assess the impact of three major parameters: dose, frequency of administration, and age at treatment initiation on therapeutic efficacy. Dose responses were simulated for all reported protocols, as shown in Fig. 1*C*. A biphasic efficacy profile was predicted to occur with all three protocols, similar to what had previously been described for mucosal insulin (36) and cholera toxin B administrations (8). Importantly, efficacy was predicted over a much larger range at lower doses for the Daniel protocol, which administered insulin peptide at less frequent dosing periods. Thus, variations in dosing protocol can impact the therapeutic dose window and pose a

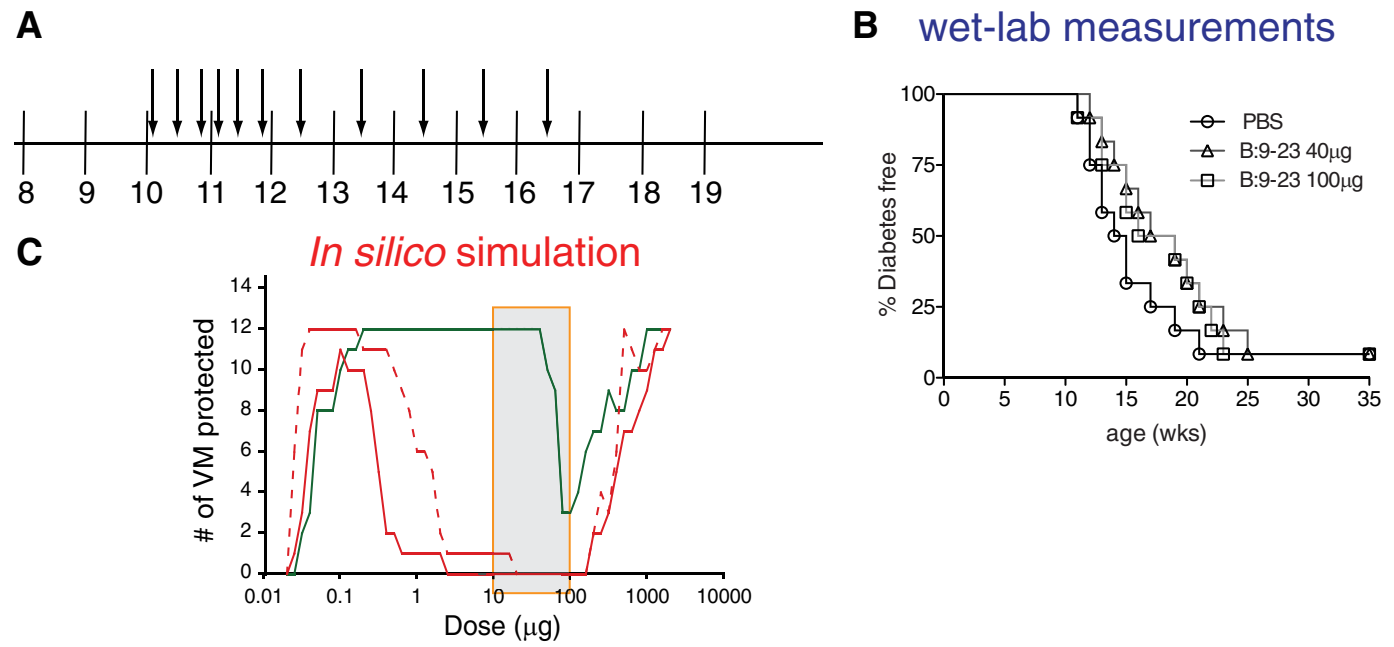

FIG. 1. Two different amounts of B:9-23 peptide cannot protect from diabetes when administered nasally in 10-week-old NOD mice. *A*: Graphic representation of the B:9-23 nasal immunization protocol followed. Ten-week-old NOD mice received 40 or 100 μg B:9-23 peptide nasal every other day for the first 2 weeks and once a week for the following 5 weeks. *B*: There was no protection from diabetes after following the protocol described in *A*. Efficacy of treatment was assessed by monitoring blood glucose over time (n = 12 in all groups). Mice were considered diabetic when blood glucose was >16.67 mmol/l for two consecutive weekly measurements. *C*: Multiphasic dose responses were predicted for the protocols presented in supplementary Table 1. Nasal B:9-23 peptide therapy was simulated for the Daniel (green solid line), Kobayashi (red solid line), and von Herrath (red dashed line) protocols across a wide range of doses (x-axis). The shaded box indicates the peptide range (10–100 μg) used to calibrate the VM. Efficacy represents the number of VM that were protected from diabetes.

significant challenge for clinical translation. Although all protocols were predicted to be effective at much higher doses, solubility concerns will preclude using such doses experimentally. Efficacy of nasal B:9-23 was predicted to decrease if treatment was started at a later age (supplementary Fig. 1*A* and *B*). To test this prediction, the Daniel protocol was initiated in vivo in older NOD mice, at 9 weeks of age. Treatments that began at 9 instead of 4 weeks of age showed a lesser protective effect (supplementary Fig. 1*C*), consistent with the simulation results.

More frequent immunization is predicted to interfere with efficient Treg induction that is required to protect from type 1 diabetes. Three major cell populations contributing to disease pathogenesis are represented in the PhysioLab platform: Th1, Th2 cells, and Treg (supplementary Table 2). Both adaptive (aTreg) and natural (nTreg) are represented, with aTreg comprising characteristics of both Tr1 and Th3 cells in the model. To gain a better understanding of the mechanisms underlying the efficacy of nasal B:9-23 therapy, we selectively turned off various of those mechanisms and reassessed the VM over a specified dose range after B:9-23 nasal immunization following the von Herrath protocol (Fig. 2*A*). At effective low doses, induction of B:9-23–specific Treg and Th2 cells were predicted to confer protection (blue line), whereas peripheral T-cell deletion (green line) was less important. Within both characterized Treg populations, nTreg induction did not seem to be important in conferring protection after nasal B:9-23 immunization, and it was induced by all three protocols in the NALT (Fig. 2*B*). In contrast, ineffective doses were predicted to be the result of aTreg deletion in the NALT because turning off this mechanism resulted in protection of all the VM (orange line). Closer looks at Treg dynamics in the model revealed that aTreg, however, was induced to a much greater extent by the effective Daniel protocol (Fig. 2*C*). More importantly, induction of aTreg by the ineffective protocols appeared to be actually hampered by the frequent, weekly immunizations, suggesting that too frequent immunizations might lead to aTreg deletion.

More frequent immunization decreases efficacy of nasal B:9-23 therapy in vivo by impairing Treg induction. To test the hypothesis that too frequent immunization is detrimental for Treg induction in vivo, mice were divided into high- and low-frequency immunization groups. Two specific immunization protocols based on predictive outputs from the platform were implemented in the wet lab, described in Table 1. No protection was predicted in any of the VM following the high-frequency protocol (Fig. 3*A*). Evaluation of the antidiabetogenic properties of B:9-23 peptide immunizations in vivo according to both protocols showed that indeed in live NOD mice the low-frequency protocol was more effective than the high-frequency one (Fig. 3*B*). In all cases, treatment was initiated at the 4-week-old periinsulitis stage, and the mice were immunized with 40 μg of B:9-23. It is important to note here that simulated responses to alternate protocols provide insight into which protocols are most robust against variability or unknowns in the underlying disease and are to be interpreted as relative ranking of protocols rather than quantitative predictions of protection.

Moreover, the PhysioLab platform predicted changes in Treg populations within the NALT, islets, blood, and PDLN, as described in Fig. 3*C*–*E*. Elevations in Treg were predicted to peak at ~1–2 weeks after each round of immunization in the NALT and blood but not in the PDLN for the low-frequency protocol (blue line). In contrast, no Treg elevation was predicted after the follow-up immunization period using the high-frequency protocol. We measured blood Treg between 10 and 12 weeks of age,

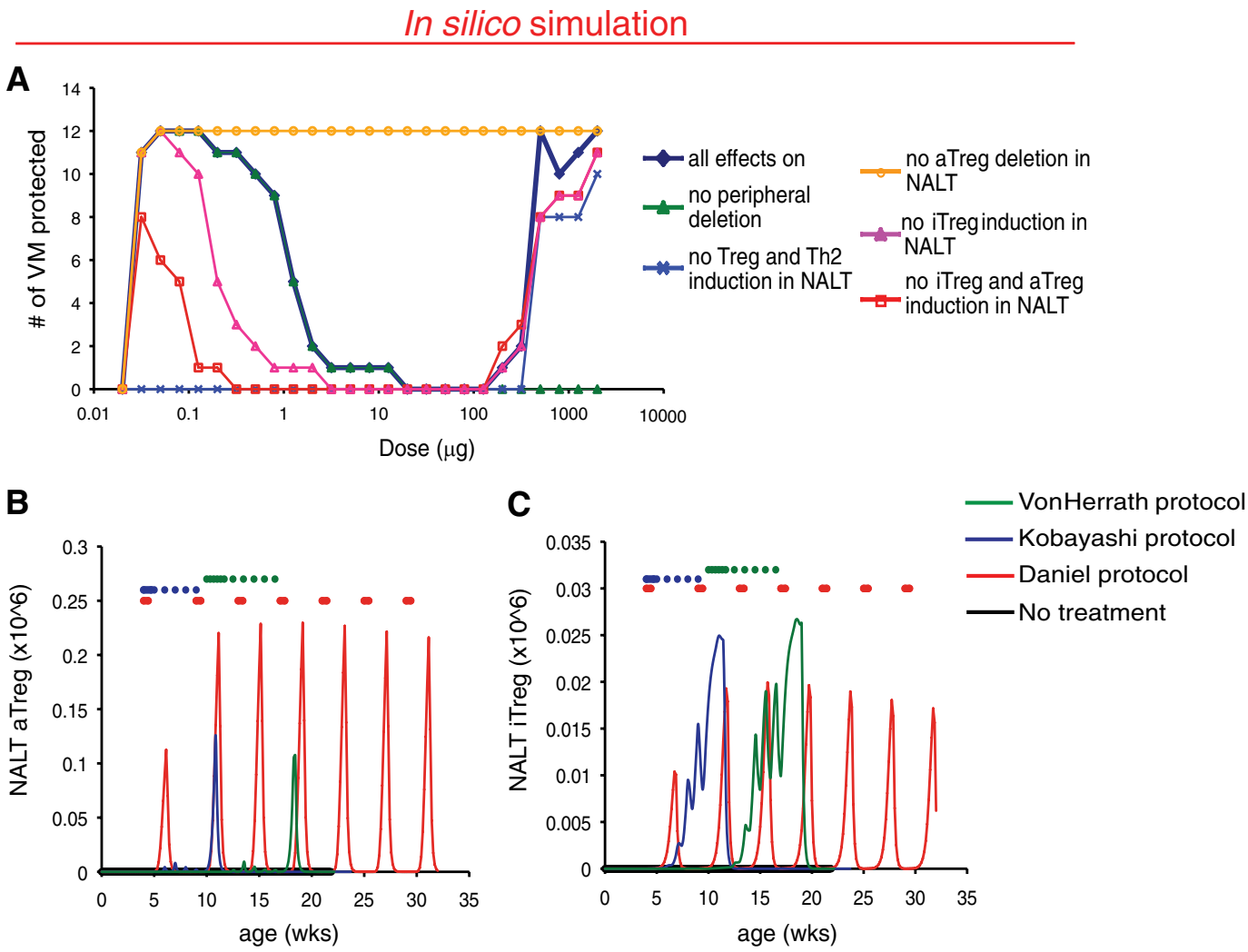

FIG. 2. Loss of efficacy after high nasal B:9–23 immunization frequency is predicted to be attributed to lower induction of aTreg in the NALT. *A*: Mechanisms driving predicted efficacy differ at low and high doses. Nasal insulin B:9-23 peptide therapy was simulated and protection from diabetes assessed using the von Herrath protocol over a dose range with various pharmacokinetic effects (PK) turned off. Only results with differences from control (all effects on) are shown. *B* and *C*: Increased immunization frequency is associated with lower induction of aTreg in the NALT. Time of administration for each protocol is indicated by colored dots. Model readouts for NALT aTreg (*B*) and nTreg (*C*) cells were assessed for each protocol (black, untreated; red, Daniel protocol; blue, Kobayashi protocol; green, von Herrath protocol). A single representative VM is shown.

corresponding to 1–3 weeks after immunization in order to test predictions of the model. In agreement with the in silico predictions, elevated Treg frequency defined as $CD4^+CD25^+Foxp3^+$ (37) was observed at weeks 10 and 11 in the blood of mice immunized with the low-frequency protocol (Fig. 3*F–H*). Interestingly, we also observed in these wet-lab studies that reduced Treg expansion occurred as a result of more frequent dosing, which was associated with lack of protection from diabetes. In addition, no significant differences were observed for Treg levels in the PDLN (Fig. *3G*). Altogether, these results provide additional confidence in the model and suggest that Treg induction and subsequently protection from diabetes in the NOD mice by nasal B:9-23 administration will perhaps more easily occur in vivo when a lower-frequency immunization protocol is chosen.

Lower frequency of nasal B:9-23 immunization decreases insulitis and increases Treg frequency within the inflamed islets. To determine the extent of islet infiltration following nasal B:9-23 immunization, pancreata from nondiabetic mice of all treatment groups were histologically examined at 12 weeks of age. As shown in Fig.

TABLE 1
Nasal B:9-23 peptide protocols optimized and recommended by the type 1 diabetes PhysioLab platform

	Initial treatment			Follow-up treatment			
Protocol	Age (weeks)	Dose (μg)	Schedule	Age (weeks)	Dose (μg)	Schedule	In silico prediction
Low frequency	4	40	3 consecutive days	9 and 13	40	3 consecutive days	Protective
High frequency	4	40	3 consecutive days	9, 10, 11, 12, and 13	40	3 consecutive days	Not protective

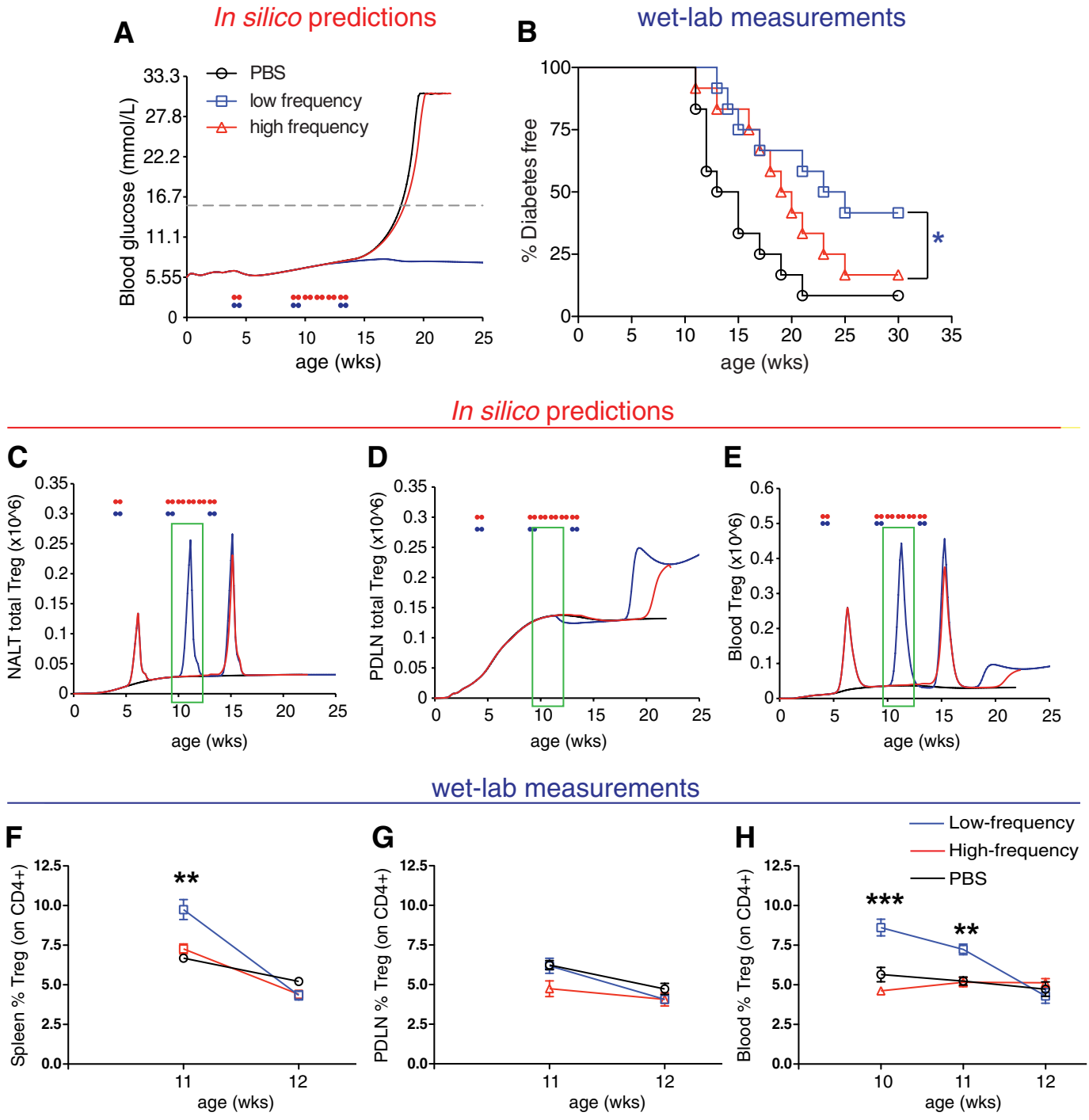

FIG. 3. Validation of predicted nasal B:9-23 immunization frequency influence on diabetes incidence and Treg levels by laboratory measurements. *A* and *B*: High-frequency immunization decreases efficacy. *A*: In silico simulation showing expected impact on blood glucose (mmol/l) in a representative virtual NOD mouse. *B*: Nasal B:9-23 administration upon low-frequency immunization protects from type 1 diabetes. Percentage of mice developing diabetes after high- or low-frequency immunizations started at 4 weeks of age with 40 mg B:9-23 peptide. At least 12 mice were included in each experimental group. Each immunization protocol was repeated in at least two independent experiments. *$P < 0.05$ between immunization groups. *C–E*: High-frequency immunization is predicted to decrease efficacy because of the deletion of aTreg in the NALT. Simulation results for Treg levels in the NALT (*C*), PDLN (*D*), and peripheral blood (*E*) in a representative VM. The green boxes indicate the suggested-by-the-model-age window at which the laboratory measurements should be conducted. *F–H*: Nasal B:9-23 administration upon low-frequency immunization induces Treg and protects from type 1 diabetes. Treg frequency (%$CD25^+Foxp3^+$ gated on $CD4^+CD127^{low}$, >95% of $CD4^+$ were $CD127^{low}$) in the spleen (*F*), PDLN (*G*), and blood (*H*) over time after high- or low-frequency immunizations ($n = 4$ mice per group). *$P < 0.05$; **$P < 0.01$; ***$P < 0.005$ between immunization groups. Data are means ± SE.

4*A–C*, the majority of islets in animals treated with the low-frequency protocol was minimally inflamed or had mild peri-insulitis. In contrast, most of the islets of normoglycemic mice that received the high-frequency immunization protocol had much greater $CD4^+$ and $CD8^+$ T-cell infiltrates. Furthermore, when scoring of the islets was undertaken, mice that received the high-frequency protocol showed a relatively greater degree of insulitis than the control mice.

Intra-islet Treg numbers were predicted to be increased

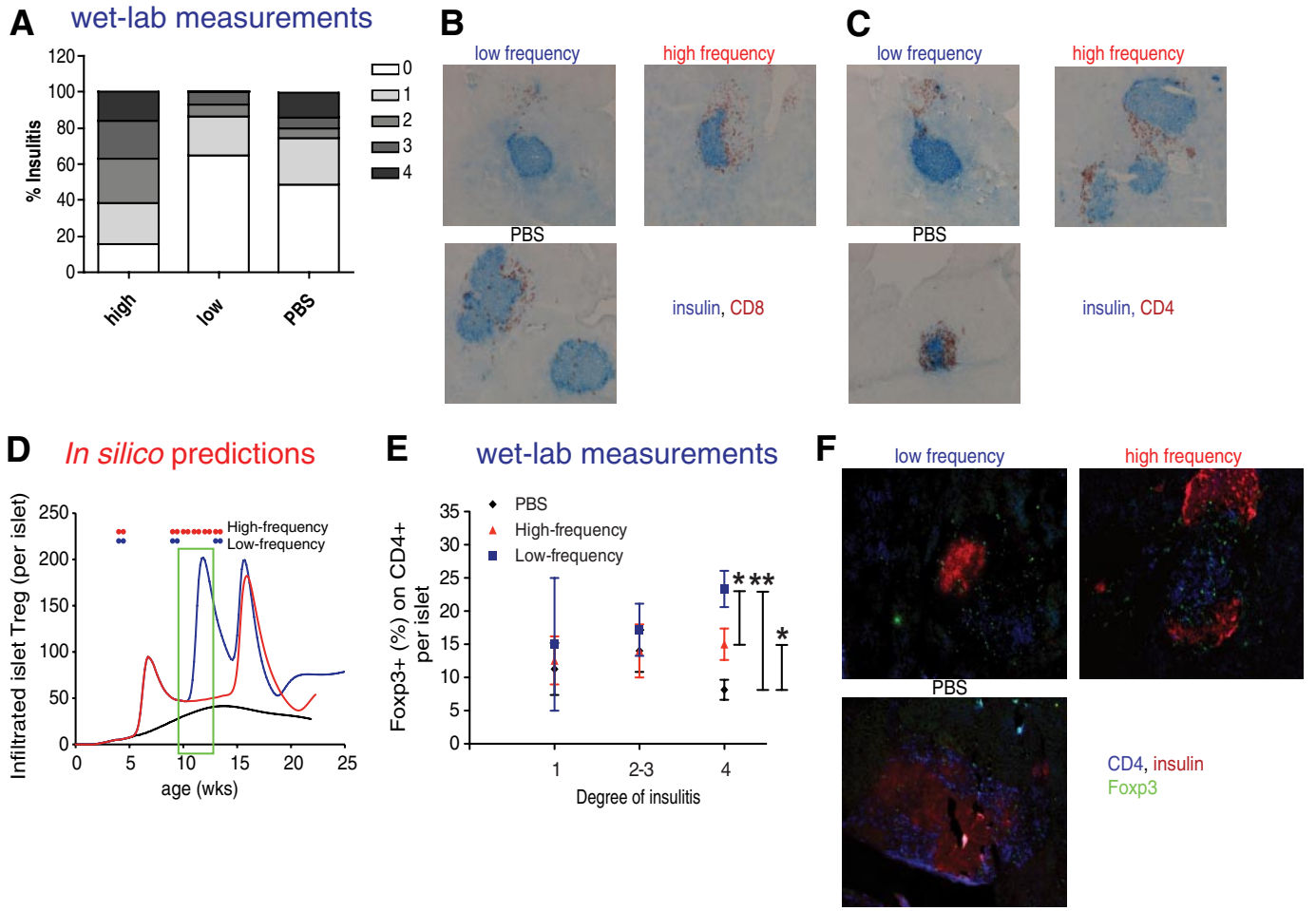

FIG. 4. Nasal B:9–23 administration started at 4 weeks of age upon low-frequency immunization decreases insulitis and increases Treg in the islets. *A–C*: Reduced insulitis in low-frequency B:9-23 nasal immunized NOD. *A*: Pancreatic sections from B:9-23 nasally treated and control (PBS) mice were scored as described in RESEARCH DESIGN AND METHODS. The percentages represent the number of islets of a given score over the total number of islets examined. Scoring was performed on histological sections derived from 12-week-old nondiabetic mice (n = 4 mice per group). *B*: Pancreatic histology. Pancreatic sections (6 μm thick) were stained for insulin (blue) and CD8 (red) (*C*) or CD4 (red) (*D*) and analyzed at ×10 magnification. All histological sections shown were derived from 12-week-old nondiabetic mice. *D–F*: Increased Treg numbers in the islets of B:9-23–immunized mice. *D*: In silico–predicted changes in Treg levels within the pancreatic islet. The green box indicates the suggested-by-the-model-age window at which the laboratory measurements should be conducted. *E*: Actual Treg frequency as determined by measuring Foxp3$^+$ cells per CD4$^+$ cells per islet according to degree of insulitis. Same histological sections as in *B* and *C* were analyzed after immunofluorescent staining (IFS) for CD4, insulin, and Foxp3. Data are means ± SE. *F*: Representative microphotograph from each group of mice with insulitis degree 4 is shown at ×20 magnification (IFS for CD4 in blue, insulin in red, and Foxp3 in green). *P < 0.05 between PBS and high-frequency, high-frequency versus low-frequency immunization. **P < 0.01 between PBS and low-frequency immunization. (A high-quality digital representation of this figure is available in the online issue.)

after the low-frequency, but not the high-frequency, immunization protocol (Fig. 4*D*). To selectively identify and quantify Treg within the islets, immunofluorescent staining for the presence of Foxp3$^+$ cells was conducted in pancreatic sections. Interestingly, highly inflamed islets with a high Treg density were indicative of treatment success. In the low-frequency treatment group, a remarkable increase in Treg density, particularly in islets with high degree of inflammation (score >3), was seen (Fig. 4*E* and *F*) (islets with similar degree of inflammation were compared between groups). Therefore, after B:9-23 nasal treatment, a relatively linear correlation between degree of insulitis and Treg frequency was observed: the higher the inflammation, the more Foxp3$^+$ cells present, with frequency that exceeded 20%. In contrast, in untreated mice a slight decline in Foxp3$^+$ cells frequency in islets with higher degree of inflammation was observed. This may be because of an inherent defect in expressing sufficient amounts of CD25 and Bcl-2, resulting in early cell death (38).

Prediction and validation of increased islet levels of IL-10 following the low-frequency protective B:9-23 immunization protocol. Simulation results predicted an elevation in IL-10 and IL-4 but a decline in IFNγ intra-islet cytokine levels at 11–12 weeks of age following the low-frequency immunization protocol (Fig. 5*A–C*). On the other hand, for the same time point, in mice immunized with the high-frequency protocol, predictions showed reduced intra-islet IL-10 levels. To test these predictions, IL-10, IL-4, and IFNγ were measured by ELIspot immunoassay. Although IL-17 was shown to be involved in hindering nasal peptide tolerance induction in experimental autoimmune encephalomyelitis (39), here it was not modeled due to its insufficient knowledge in diabetes pathogenesis. Interestingly, as shown in Fig. 5*D* and *E*, an increase of IL-10 production in the intra-islet–derived lymphocytes was observed. Similarly in the PDLN, as shown in Fig. 6*C*, IL-10 levels were increased, whereas IL-4 levels were slightly but not significantly higher in the blood and spleen of mice that had received the low-frequency protocol. Moreover, IL-4

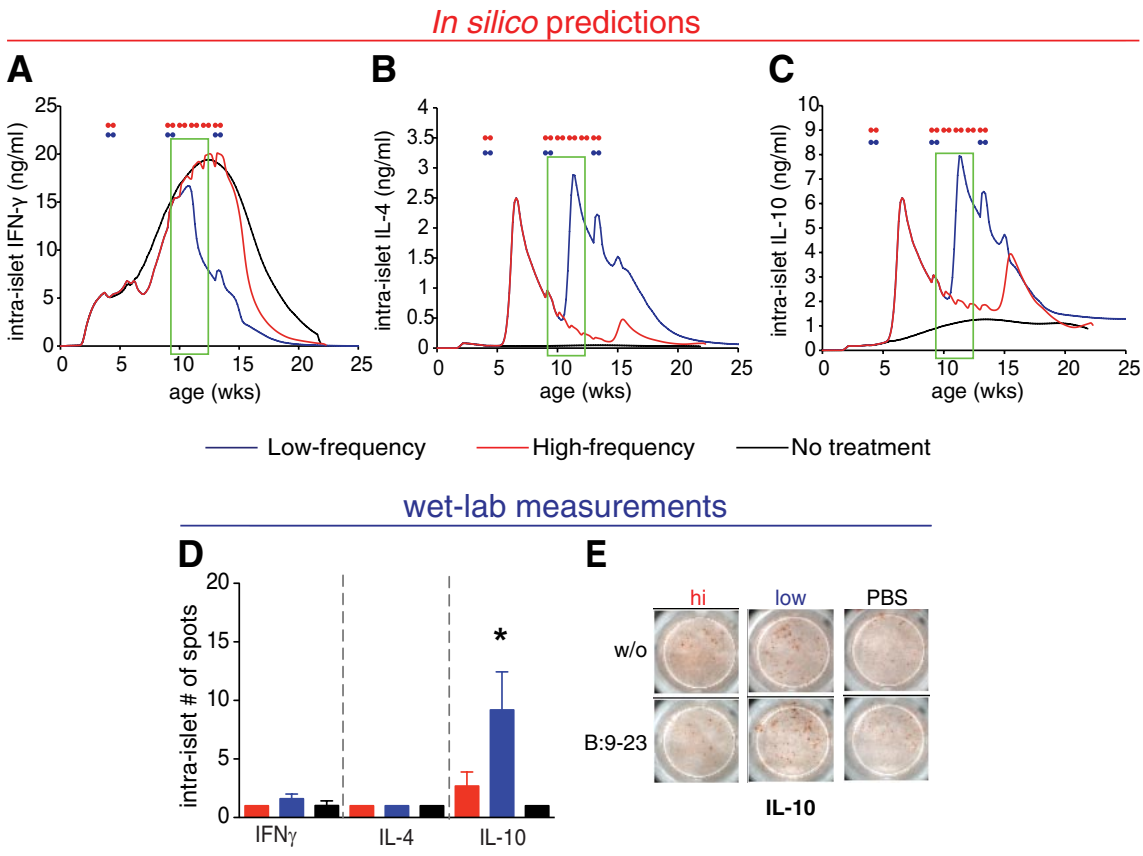

FIG. 5. Validation of the predicted changes in intra-islet IL-10 cytokine levels after nasal B:9-23 immunization by laboratory measurements. *A–C*: Low-frequency immunization is predicted to decrease IFNγ and increase IL-10 levels in the pancreas. Simulation for intra-islet levels for IFNγ (*A*), IL-4 (*B*), and IL-10 (*C*) over time in VM treated with either low-frequency (blue) or high-frequency (red) nasal B:9-23 protocol. The green boxes indicate the suggested-by-the-model-age window at which the laboratory measurements should be conducted. *D* and *E*: Laboratory measurements show an increase in IL-10 levels in the intra-islet lymphocytes isolated from the pancreas of 12-week-old mice. *D*: Number of B:9-23–reactive per 2.5 × 10^5 T-cells producing IFNγ, IL-4, and IL-10 in pancreas (intra-islet) from treated and control mice following B:9-23 in vitro restimulation. ELIspot was performed after 3 days in vitro stimulation in the presence of 10 μg/ml B:9-23 and 50 μ/ml rhIL-2. The bars represent the average of antigen-specific responder cells after subtracting the background (without [w/o] stimulation) (n = 4 mice per group) ± SE. *P < 0.05 between high-frequency and low-frequency immunization. *E*: Representative spot pictures for IL-10 assayed in the pancreas. (A high-quality digital representation of this figure is available in the online issue.)

levels between untreated and low-frequency–treated mice were not different. Unexpectedly, IFNγ was elevated with the low-frequency protocol particularly in the spleen Fig. 6*A*. This observation could reflect the unconventional protective role for IFNγ, whereby IFNγ may suppress pathogenic IL-17 producing T-cells (40).

Further in silico analysis suggested that effective nasal B:9-23 treatment should be most sensitive to IL-10 and

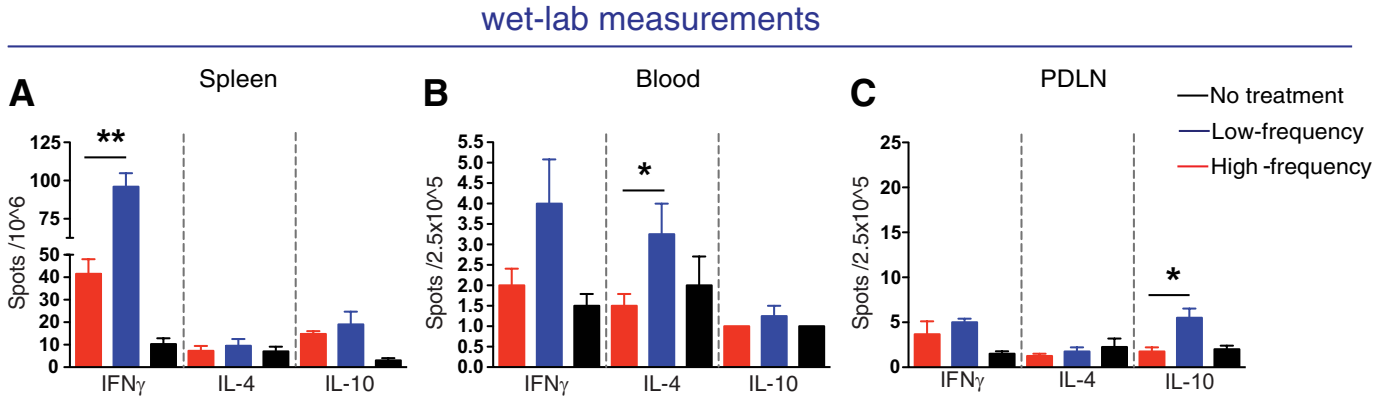

FIG. 6. Increased IFNγ cytokine levels in the spleen and IL-10 levels in the PDLN after low nasal B:9-23 immunization. *A–C*: Laboratory measurements suggest an increase in IFNγ levels and IL-10 in the spleen and PDLN, respectively. Number of B:9-23–reactive T-cells producing IFNγ, IL-4, and IL-10 in the spleen (*A*), blood (*B*), and PDLN (*C*) of B:9-23 nasal-treated and control mice following B:9-23 in vitro restimulation after subtracting the background (without stimulation). ELIspot was performed using CD8-depleted splenocytes from 12-week-old mice stimulated in vitro for 3 days in the presence of 10 μg/ml B:9-23 and 50 μ/ml rhIL-2. The bars represent the average ±SE of antigen-specific responding cells (n = 4 mice per group).

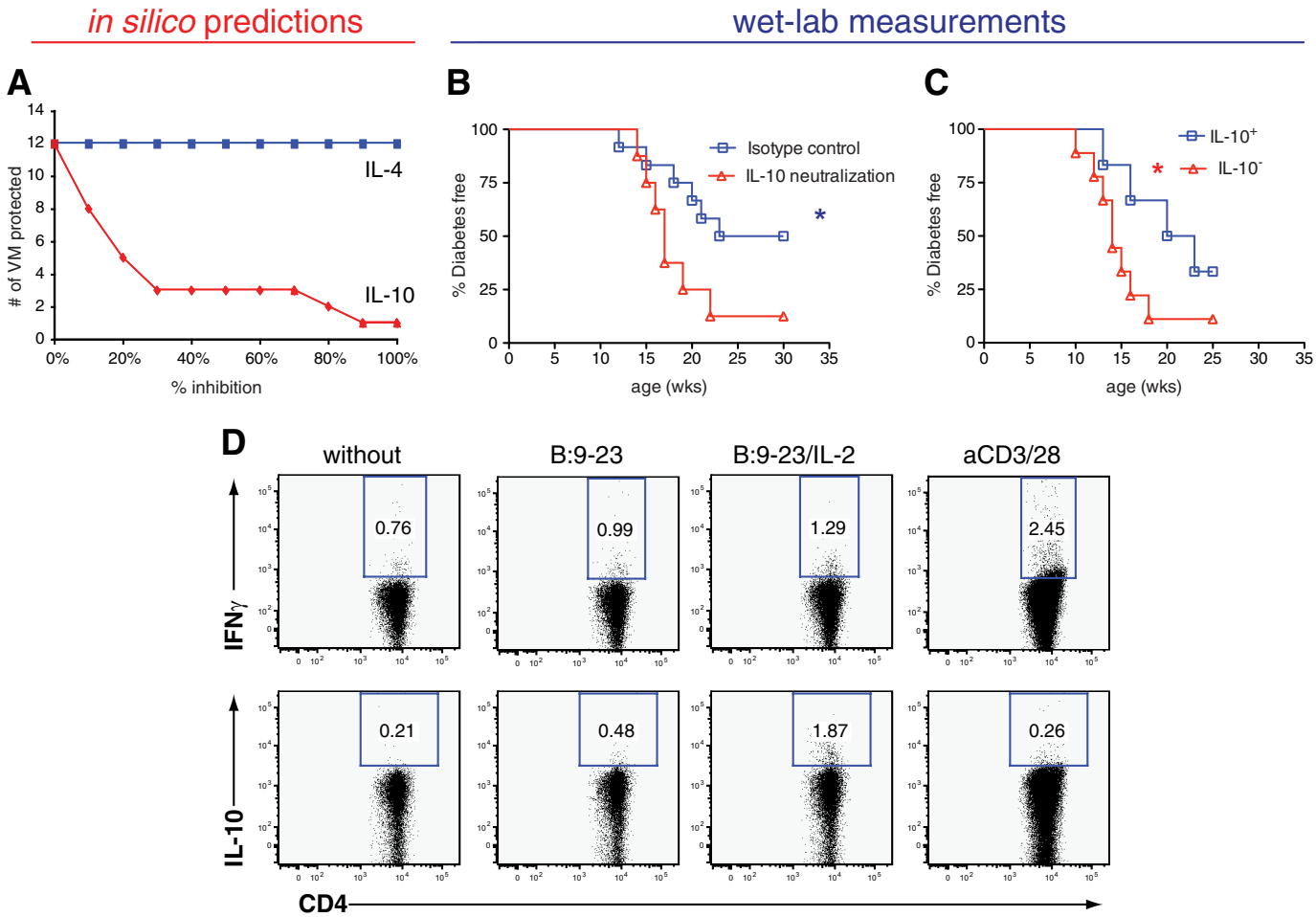

FIG. 7. In silico analysis predicts and laboratory measurements verify that IL-10 is the major cytokine mediator in achieving tolerance after nasal B:9-23 low-frequency immunization. *A*: Efficacy of nasal B:9-23 treatment is most sensitive to inhibition by IL-10, whereas negligible sensitivity to IL-4 is predicted. Low-frequency immunization was simulated in VM where IL-10 (blue) or IL-4 (red) was inhibited from 0 to 100%. *B*: IL-10 neutralization inhibits nasal B:9-23 tolerogenic effect. Live NOD mice treated with the low-frequency immunization protocol were divided in two groups. One group received anti–IL-10 neutralizing antibody, while in the second group the isotype antibody control was administered. Treatments were initiated at 4 weeks of age. Anti–IL-10 or isotype control was given to the mice (125 μg/mouse per injection) intraperitoneally twice a week at 5, 6, 10, 11, 14, and 15 weeks of age. The mice received a total of eight antibody injections. At least eight mice were included per experimental group (*$P < 0.05$). Mice receiving anti–IL-10 alone without the peptide treatment showed similar type 1 diabetes progression to the ones being completely unmanipulated (data not shown). *C* and *D*: IL-10–producing cells induced after nasal B:9-23 treatment mediate the protection. CD8-depleted cells from B:9-23–immunized and –protected mice were pooled together and cultured in the presence of B:9-23 (10 μg/ml) and rhIL-2 (50 units/ml) for 3 days. Subsequently, cells were assayed for cytokine production by intracellular cytokine staining after restimulation with anti-CD3/anti-CD28 or B:9-23 with or without rhIL-2 and fresh TDS (gate on $CD4^+$). *D*: $IL\text{-}10^+$ and $IL\text{-}10^-$ cells ($\sim 10^6$) were prepared with the Miltenyi kit after restimulation with fresh TDS, B:9-23, and rhIL-2. *C*: Cells were transferred into 6- to 8-week-old prediabetic hosts in three independent experiments with two to three mice per group. Diabetes incidence was followed for up to 30 weeks of age, and the results shown are cumulative with at least six mice per group.

with negligible sensitivity to IL-4 (Fig. 7*A*). Therefore, to test the importance of IL-10 in B:9-23–mediated tolerance, mice receiving the low-frequency protocol were treated intraperitoneally with anti–IL-10 neutralizing antibody. Given that the model predicts a delay of 1–2 weeks after nasal immunization for aTreg (Fig. 2*C*) and IL-10 levels (Fig. 5*C*) to increase, anti–IL-10 was administered in vivo 1 and 2 weeks after each nasal immunization (i.e., at 5, 6, 10, 11, 14, and 15 weeks of age). In vivo IL-10 neutralization abrogated the nasal B:9-23 protective effect as shown in Fig. 7*B*. Interestingly, IL-10 neutralizing antibody had to be administered after each round of nasal B:9-23 treatment, and normal progression to diabetes was not restored when it was only administered at 10 and 11 weeks of age, while anti–IL-10 treatment alone slightly but not significantly increased disease progression in untreated NOD mice (data not shown).

Further adoptive transfer studies shown in Fig. 7*C* and *D* confirmed that IL-10–producing Treg could transfer protection following nasal B:9-23 treatment. In these studies, $CD4^+$ T-cells derived from normoglycemic ~30-week-old nasal B:9-23–protected mice were activated with B:9-23 and IL-2 in vitro leading to a significant number (2%) of $IL\text{-}10^+$ B:9-23–specific cells. $IL\text{-}10^+$ cells were purified and adoptively transferred into nonimmunized 6- to 8-week-old NOD hosts. Importantly, short-term protection was only conveyed by the $IL\text{-}10^+$ Treg (Fig. 7*C*). Altogether, these results demonstrate that IL-10 is essential for protection from diabetes after nasal B:9-23 treatment, thus confirming our in silico predictions.

DISCUSSION

Although many approaches to induce antigen-specific tolerance to prevent type 1 diabetes have been successful in the NOD mouse, translating these strategies to humans has been challenging given the multitude of variables that can affect the outcome (41). In NOD mice, factors related

to the precise therapeutic regimen are rather impractical to systematically investigate in the laboratory due to the very large number of possible combinations of multiple parameters. Furthermore, intramouse variability of disease pathogenesis even in inbred organisms presents another complicating issue necessitating the use of groups with large numbers of mice. Last, development of reliable biomarkers that, for example, would track the successful induction of Treg at the correct time postimmunization has also been slow, because the optimal time point of sample recovery is unknown. Here, we demonstrate that biosimulation can be a useful tool to explore variations in the protocol regimen and define optimal time points to test Treg induction as well as point toward crucial biologic factors mediating tolerance. Overall, our present study demonstrates that simulation results can be used to focus and guide laboratory experiments and optimize treatment regimens for type 1 diabetes. Our in silico simulation investigated the effect of dose, frequency, and age at initiation on the efficacy of nasal B:9-23 treatment in a cohort of VM. Nasal B:9-23 immunization appeared to be efficacious at low and high doses but not at intermediate doses. With respect to age, efficacy was generally predicted to be biphasic and better when treatment was started earlier. In addition, and possibly of high importance for ongoing nasal insulin trials, in silico analysis predicted that too frequent immunization was ineffective, while lower immunization frequency induced increased IL-10 levels and aTreg induction. This resulted in a much larger efficacious dose range for lower insulin doses that lead to efficient Treg induction. In other words, by reducing the frequency of insulin administration, even higher doses could still result in tolerance. This might have important implications for human trials with nasal and oral insulin, where the optimal efficacious dose is still unknown but where the immunization frequency could be reduced.

The in silico prediction that too frequent immunization can be detrimental was corroborated by subsequent in vivo experiments. Furthermore, the predicted underlying mechanism of increasing Treg levels with low-frequency dosing was also confirmed, as was the association with higher IL-10 levels in the pancreas. Moreover, in vivo blockade of IL-10 and adoptive transfer of B:9-23–specific IL-10–producing Treg attributed a key role to this cytokine in nasal B:9-23 therapy. Interestingly, the role of IL-10, derived by induced Tr1/Th3 cells or $CD4^+CD25^+Foxp3^+$ aTreg in nasal autoantigen-induced tolerance, has been described before (42–44). Here, we cannot dissect the relative involvement of both cell populations in establishing nasal tolerance, as the aTreg representation in the model is generic to encompass characteristics of Tr1 and Th3 cells. Although further experimentation is necessary to thoroughly address each mechanism, our results provide evidence that the top-down approach to modeling disease we applied had sufficient detail to be predictive.

While our laboratory experiments provided additional validation for the predictive capacity of the type 1 diabetes PhysioLab platform, not all model predictions were consistent with laboratory experiments (summarized in supplementary Table 4). For example, Treg frequency in the pancreas was predicted to be increased predominantly by the low-frequency protocol at the time point indicated but was actually elevated by both low- and high-frequency protocols compared with controls. However, high-frequency immunization induced increased insulitis, whereas it delayed type 1 diabetes progression to a limited degree. Presumably, the high degree of lymphocytic infiltration was counterregulated by an increased frequency of Tregs in the islets in this scenario. Since mucosal autoantigen administration can at very high doses induce cytotoxic T-cell responses accelerating type 1 diabetes onset in mice (45), caution should be taken when applying antigen-specific immunotherapy at very high dosages or very high frequencies, or both, for the treatment of human autoimmune disease. While our top-down modeling approach is not infallible and has some deficiencies and inaccuracies, it is still able to have good predictive capacity. As modeling is an iterative process, these discordant data may be incorporated into the next generation of VM to build upon and enhance the predictive capacity of the model.

The wet-lab observation that low-frequency dosing may increase IFNγ levels in the spleen also suggested that IFNγ might have a yet unappreciated role in type 1 diabetes in the NOD mouse. A recent report (40) indicated that IFNγ could, by reducing IL-17, have a protective role in autoimmune diabetes. The current version of the platform assumes that IFNγ has only pathogenic effects and does not have a representation for IL-17. This illustrates the need for future expansion of the platform to include alternative functions of IFNγ, and perhaps representation of Th17 cells and IL-17, to explore the potential impact of this biology as its role in type 1 diabetes continues to emerge. Overall, we can see here that one of the strengths of the top-down modeling approach is that it can be predictive despite lacking every possible detail. This study demonstrates the utility of mechanism-based biosimulation methods to efficiently optimize dosing schedules where the combinations of the variables that need to be tested in the laboratory render the task impractical and to provide guidance for when to measure candidate biomarkers. Our results suggest that immunization frequency should be a major consideration for ongoing clinical trials that aim to induce tolerance in humans and that IL-10 and Treg levels may be useful biomarkers to predict efficacy of treatment.

Last, humanization of the PhysioLab platform should be warranted to give guidance for improved design of future clinical trials. What we envision in humans, where type 1 diabetes is a lot more heterogeneous, is the generation of a general platform, which will be easily adapted to each individual characteristics (i.e., family history, genetic background, number and titers of autoantibodies, glycosylated hemoglobin, and C-peptide levels). Thus, personalized simulations will become possible and customized treatments would be suggested on an individual basis.

ACKNOWLEDGMENTS

This work was supported by a Juvenile Diabetes Research Foundation PPG (7-2005-877), a National Institute of Allergy and Infectious Diseases Prevention Center (U) grant, and an American Diabetes Association development grant for in silico modeling, as well as funds from the Brehm coalition. The sponsors of this study had no role in study design, data collection, data analysis, data interpretation, or writing of the report. The corresponding author had full access to all the data in the study and had final responsibility for the decision to submit for publication.

No potential conflicts of interest relevant to this article were reported.

C.J., Z.Y., and W.C. calibrated and optimized the T1D PhysioLab platform and designed and conducted all the in

silico investigation. F.G. and D.A. performed all the wet-lab experiments, which were designed by all aforementioned, including B.D., C.M., and M.v.H. F.G., C.J., and M.v.H. analyzed the results and wrote the manuscript. All authors contributed to the interpretation of the data, revised the report critically, and approved the final submission.

REFERENCES

1. Alleva DG, Crowe PD, Jin L, Kwok WW, Ling N, Gottschalk M, Conlon PJ, Gottlieb PA, Putnam AL, Gaur A. A disease-associated cellular immune response in type 1 diabetics to an immunodominant epitope of insulin. J Clin Invest 2001;107:173–180
2. Arif S, Tree TI, Astill TP, Tremble JM, Bishop AJ, Dayan CM, Roep BO, Peakman M. Autoreactive T cell responses show proinflammatory polarization in diabetes but a regulatory phenotype in health. J Clin Invest 2004;113:451–463
3. Achenbach P, Koczwara K, Knopff A, Naserke H, Ziegler AG, Bonifacio E. Mature high-affinity immune responses to (pro)insulin anticipate the autoimmune cascade that leads to type 1 diabetes. J Clin Invest 2004;114:589–597
4. Di Lorenzo TP, Peakman M, Roep BO. Translational mini-review series on type 1 diabetes: systematic analysis of T cell epitopes in autoimmune diabetes. Clin Exp Immunol 2007;148:1–16
5. Nakayama M, Abiru N, Moriyama H, Babaya N, Liu E, Miao D, Yu L, Wegmann DR, Hutton JC, Elliott JF, Eisenbarth GS. Prime role for an insulin epitope in the development of type 1 diabetes in NOD mice. Nature 2005;435:220–223
6. Nakayama M, Babaya N, Miao D, Gianani R, Liu E, Elliott JF, Eisenbarth GS. Long-term prevention of diabetes and marked suppression of insulin autoantibodies and insulitis in mice lacking native insulin B9–23 sequence. Ann N Y Acad Sci 2006;1079:122–129
7. Nakayama M, Beilke JN, Jasinski JM, Kobayashi M, Miao D, Li M, Coulombe MG, Liu E, Elliott JF, Gill RG, Eisenbarth GS. Priming and effector dependence on insulin B:9–23 peptide in NOD islet autoimmunity. J Clin Invest 2007;117:1835–1843
8. Aspord C, Thivolet C. Nasal administration of CTB-insulin induces active tolerance against autoimmune diabetes in non-obese diabetic (NOD) mice. Clin Exp Immunol 2002;130:204–211
9. Daniel D, Wegmann DR. Protection of nonobese diabetic mice from diabetes by intranasal or subcutaneous administration of insulin peptide B-(9–23). Proc Natl Acad Sci U S A 1996;93:956–960
10. Every AL, Kramer DR, Mannering SI, Lew AM, Harrison LC. Intranasal vaccination with proinsulin DNA induces regulatory CD4+ T cells that prevent experimental autoimmune diabetes. J Immunol 2006;176:4608–4615
11. Harrison LC, Dempsey-Collier M, Kramer DR, Takahashi K. Aerosol insulin induces regulatory CD8 gamma delta T cells that prevent murine insulin-dependent diabetes. J Exp Med 1996;184:2167–2174
12. Kobayashi M, Abiru N, Arakawa T, Fukushima K, Zhou H, Kawasaki E, Yamasaki H, Liu E, Miao D, Wong FS, Eisenbarth GS, Eguchi K. Altered B:9–23 insulin, when administered intranasally with cholera toxin adjuvant, suppresses the expression of insulin autoantibodies and prevents diabetes. J Immunol 2007;179:2082–2088
13. Liu E, Abiru N, Moriyama H, Miao D, Eisenbarth GS. Induction of insulin autoantibodies and protection from diabetes with subcutaneous insulin B:9–23 peptide without adjuvant. Ann N Y Acad Sci 2002;958:224–227
14. Martinez NR, Augstein P, Moustakas AK, Papadopoulos GK, Gregori S, Adorini L, Jackson DC, Harrison LC. Disabling an integral CTL epitope allows suppression of autoimmune diabetes by intranasal proinsulin peptide. J Clin Invest 2003;111:1365–1371
15. Alleva DG, Gaur A, Jin L, Wegmann D, Gottlieb PA, Pahuja A, Johnson EB, Motheral T, Putnam A, Crowe PD, Ling N, Boehme SA, Conlon PJ. Immunological characterization and therapeutic activity of an altered-peptide ligand, NBI-6024, based on the immunodominant type 1 diabetes autoantigen insulin B-chain (9–23) peptide. Diabetes 2002;51:2126–2134
16. Liu E, Moriyama H, Paronen J, Abiru N, Miao D, Yu L, Taylor RM, Eisenbarth GS. Nondepleting anti-CD4 monoclonal antibody prevents diabetes and blocks induction of insulin autoantibodies following insulin peptide B:9–23 immunization in the NOD mouse. J Autoimmun 2003;21:213–219
17. Mukherjee R, Chaturvedi P, Qin HY, Singh B. CD4+CD25+ regulatory T cells generated in response to insulin B:9–23 peptide prevent adoptive transfer of diabetes by diabetogenic T cells. J Autoimmun 2003;21:221–237
18. Urbanek-Ruiz I, Ruiz PJ, Paragas V, Garren H, Steinman L, Fathman CG. Immunization with DNA encoding an immunodominant peptide of insulin prevents diabetes in NOD mice. Clin Immunol 2001;100:164–171
19. Chaillous L, Lefevre H, Thivolet C, Boitard C, Lahlou N, Atlan-Gepner C, Bouhanick B, Mogenet A, Nicolino M, Carel JC, Lecomte P, Marechaud R, Bougneres P, Charbonnel B, Sai P. Oral insulin administration and residual beta-cell function in recent-onset type 1 diabetes: a multicentre randomised controlled trial: Diabete Insuline Orale group. Lancet 2000;356:545–549
20. Harrison LC, Honeyman MC, Steele CE, Stone NL, Sarugeri E, Bonifacio E, Couper JJ, Colman PG. Pancreatic β-cell function and immune responses to insulin after administration of intranasal insulin to humans at risk for type 1 diabetes. Diabetes Care 2004;27:2348–2355
21. Kupila A, Sipila J, Keskinen P, Simell T, Knip M, Pulkki K, Simell O. Intranasally administered insulin intended for prevention of type 1 diabetes: a safety study in healthy adults. Diabetes Metab Res Rev 2003;19:415–420
22. Pozzilli P, Pitocco D, Visalli N, Cavallo MG, Buzzetti R, Crino A, Spera S, Suraci C, Multari G, Cervoni M, Manca Bitti ML, Matteoli MC, Marietti G, Ferrazzoli F, Cassone Faldetta MR, Giordano C, Sbriglia M, Sarugeri E, Ghirlanda G. No effect of oral insulin on residual beta-cell function in recent-onset type I diabetes (the IMDIAB VII). IMDIAB Group. Diabetologia 2000;43:1000–1004
23. Skyler JS, Krischer JP, Wolfsdorf J, Cowie C, Palmer JP, Greenbaum C, Cuthbertson D, Rafkin-Mervis LE, Chase HP, Leschek E. Effects of oral insulin in relatives of patients with type 1 diabetes: the Diabetes Prevention Trial–Type 1. Diabetes Care 2005;28:1068–1076
24. Nanto-Salonen K, Kupila A, Simell S, Siljander H, Salonsaari T, Hekkala A, Korhonen S, Erkkola R, Sipila JI, Haavisto L, Siltala M, Tuominen J, Hakalax J, Hyoty H, Ilonen J, Veijola R, Simell T, Knip M, Simell O. Nasal insulin to prevent type 1 diabetes in children with HLA genotypes and autoantibodies conferring increased risk of disease: a double-blind, randomised controlled trial. Lancet 2008;372:1746–1755
25. Fousteri G, von Herrath M, Bresson D. Mucosal exposure to antigen: cause or cure of type 1 diabetes?. Curr Diab Rep 2007;7:91–98
26. Miller SD, Turley DM, Podojil JR. Antigen-specific tolerance strategies for the prevention and treatment of autoimmune disease. Nat Rev Immunol 2007;7:665–677
27. Zheng Y, Kreuwel HT, Young DL, Shoda LK, Ramanujan S, Gadkar KG, Atkinson MA, Whiting CC. The virtual NOD mouse: applying predictive biosimulation to research in type 1 diabetes. Ann N Y Acad Sci 2007;1103:45–62
28. Shoda L, Kreuwel H, Gadkar K, Zheng Y, Whiting C, Atkinson M, Bluestone J, Mathis D, Young D, Ramanujan S. The type 1 diabetes PhysioLab platform: a validated physiologically based mathematical model of pathogenesis in the non-obese diabetic mouse. Clin Exp Immunol 2010;161:250–267
29. Tree TI, Lawson J, Edwards H, Skowera A, Arif S, Roep BO, Peakman M. Naturally arising human CD4 T-cells that recognize islet autoantigens and secrete interleukin-10 regulate proinflammatory T-cell responses via linked suppression. Diabetes 59:1451–1460
30. Achenbach P, Barker J, Bonifacio E. Modulating the natural history of type 1 diabetes in children at high genetic risk by mucosal insulin immunization. Curr Diab Rep 2008;8:87–93
31. Orban T, Farkas K, Jalahej H, Kis J, Treszl A, Falk B, Reijonen H, Wolfsdorf J, Ricker A, Matthews JB, Tchao N, Sayre P, Bianchine P. Autoantigen-specific regulatory T cells induced in patients with type 1 diabetes mellitus by insulin B-chain immunotherapy. J Autoimmun 2009;34:408–415
32. Staeva-Vieira T, Peakman M, von Herrath M. Translational mini-review series on type 1 diabetes: Immune-based therapeutic approaches for type 1 diabetes. Clin Exp Immunol 2007;148:17–31
33. Metzler B, Anderton SM, Manickasingham SP, Wraith DC. Kinetics of peptide uptake and tissue distribution following a single intranasal dose of peptide. Immunol Invest 2000;29:61–70
34. Fousteri G, Dave A, Bot A, Juntti T, Omid S, von Herrath M. Subcutaneous insulin B:9–23/IFA immunisation induces Tregs that control late-stage prediabetes in NOD mice through IL-10 and IFNgamma. Diabetologia 2010;53:1958–1970
35. Bresson D, Fradkin M, Manenkova Y, Rottembourg D, von Herrath M. Genetic-induced variations in the GAD65 T-cell repertoire governs efficacy of anti-CD3/GAD65 combination therapy in new-onset type 1 diabetes. Mol Ther 18:307–316
36. Homann D, Holz A, Bot A, Coon B, Wolfe T, Petersen J, Dyrberg TP, Grusby MJ, von Herrath MG. Autoreactive CD4+ T cells protect from autoimmune diabetes via bystander suppression using the IL-4/Stat6 pathway. Immunity 1999;11:463–472
37. Tian B, Hao J, Zhang Y, Tian L, Yi H, O'Brien TD, Sutherland DE, Hering BJ, Guo Z. Upregulating CD4+CD25+FOXP3+ regulatory T cells in pancreatic lymph nodes in diabetic NOD mice by adjuvant immunotherapy. Transplantation 2009;87:198–206

38. Tang Q, Adams JY, Penaranda C, Melli K, Piaggio E, Sgouroudis E, Piccirillo CA, Salomon BL, Bluestone JA. Central role of defective interleukin-2 production in the triggering of islet autoimmune destruction. Immunity 2008;28:687–697
39. Wang GY, Sun B, Kong QF, Zhang Y, Li R, Wang JH, Wang DD, Lv GX, Li HL. IL-17 eliminates the therapeutic effects of myelin basic protein-induced nasal tolerance in experimental autoimmune encephalomyelitis by activating IL-6. Scand. J Immunol 2008;68:589–597
40. Jain R, Tartar DM, Gregg RK, Divekar RD, Bell JJ, Lee HH, Yu P, Ellis JS, Hoeman CM, Franklin CL, Zaghouani H. Innocuous IFNgamma induced by adjuvant-free antigen restores normoglycemia in NOD mice through inhibition of IL-17 production. J Exp Med 2008;205:207–218
41. Luo X, Herold KC, Miller SD. Immunotherapy of type 1 diabetes: where are we and where should we be going?. Immunity 32:488–499
42. Barbey C, Donatelli-Dufour N, Batard P, Corradin G, Spertini F. Intranasal treatment withovalbumin but not the major T cell epitope ovalbumin 323–339 generates interleukin-10 secreting T cells and results in the induction of allergen systemic tolerance. Clin Exp Allergy 2004;34:654–662
43. Kaya Z, Dohmen KM, Wang Y, Schlichting J, Afanasyeva M, Leuschner F, Rose NR. Cutting edge: a critical role for IL-10 in induction of nasal tolerance in experimental autoimmune myocarditis. J Immunol 2002;168:1552–1556
44. O'Neill EJ, Day MJ, Wraith DC. IL-10 is essential for disease protection following intranasal peptide administration in the C57BL/6 model of EAE. J Neuroimmunol 2006;178:1–8
45. Blanas E, Carbone FR, Allison J, Miller JF, Heath WR. Induction of autoimmune diabetes by oral administration of autoantigen. Science 1996;274:1707–1709